Industrial Engineering Journal
ISSN: 0970-2555
Volume : 53, Issue 11, No.1, November : 2024

STUDY OF DIELECTRIC PROPERTIES OF SILVER NANO-PARTICLE DISPERSED NEMATIC LIQUID CRYSTAL 4'HEPTYL-BIPHENYLE-4-CARBONITRILE

Mr. Ankur Srivastava, **Mr. Pravesh Kumar Vishwakarma, Mr. Siddharth Pratap Singh,**
Department of Physics and Electronics, Dr. R. M. L. Avadh University, Ayodhya
Dr. Prashant Kumar Singh, Assistant Professor, Department of Applied Science & Humanities, I.E.T., Dr. R. M. L. Avadh University, Ayodhya, U.P., India
Dr. Sindhu Singh, **Dr. Anil Kumar**, Assistant Professor, Department of Physics and Electronics, Dr. R. M. L. Avadh University, Ayodhya-224001, U.P., India
Dr. Anoop K. Srivastava, Associate Professor, Department of Applied Science & Humanities, I.E.T., Dr. R. M. L. Avadh University, Ayodhya-224001, U.P., India

ABSTRACT
The dispersion of the nanoparticles to pure nematic liquid crystal (NLC) improves the liquid crystal (LC) host's physical characteristics. Dispersion of nanomaterials has an impact on LC molecules cause of local molecular configurations. The present work involve the dispersion of silver nanoparticles (Ag-NPs) in positive dielectric anisotropic nematic liquid crystal 4'-n-Heptyl-4-cyanobiphenyl (7CB) at different concentrations of 0.2, 0.4, 0.6 and 0.8 weight percent. The dielectric spectra recorded for planar (homogeneous) and vertical (homeotropic) aligned samples in frequency range 100Hz-10MHz of pure and silver nano-particle (Ag-NPs) dispersed NLC. The dielectric strength ($\Delta\varepsilon$) and relaxation frequency (f_r) are also calculated. The relaxation frequency of planer aligned sample found 700kHz, 853kHz, 1MHz, 1.03MHz and 722kHz for pure, 0.2, 0.4, 06, and 0.08wt% respectively. Similar behavior is also observed for homeotropic samples also.
Keyword: Nematic liquid crystal, dielectric strength, relaxation frequency, dielectric permittivity

1. Introduction
Liquid crystals (LCs) are a special class of soft condensed matter in which the molecules maintain a delicate balance of order and fluidity. They exhibit a number of exceptional properties that are not only fascinating from a basic science standpoint, but also have enormous potential for a variety of novel applications[1–3].The simplest of all LC phases is Nematic liquid crystal (NLC), which is widely used in liquid crystal displays (LCDs) and a variety of nondisplay applications. LCD requires technological advancements such as low power consumption, faster response time, and a wider viewing angle. In recent years, there has been a strong emphasis on tailoring the properties of liquid crystals by dispersing suitable nonmesogenic materials (dyes, polymers, nanoparticles, carbon nanotubes, quantum dot, etc) into the host LCs[4–7].

Promising materials for the display and sensor industries, fast electro-optical switchers and shutters, memory cells, tunable filters, nonlinear optical valves for optical processing systems, etc., are liquid crystals containing dispersed NPs of different sizes and shapes[8,9]. With the appropriate technologies, it is anticipated that coupling the anisotropic elasticity of LCs to the optical, conductive characteristics of NPs will provide an extra advantage[10]. Controlling the NPs interact with LC molecules is therefore essential in order to customize the macroscopic characteristics overall for particular uses. Due to their exploitable optical properties, metal NPs are widely used. Because of their conductivity, chemical stability, strong calorimetric effect at the nanoscale range and medical applications, silver (Ag) nanoparticles are among the most well-known and frequently used metal NPs [11–13]. The phase transitions, molecular alignment and other LC parameters were considerably altered when silver nanoparticles were added to a pure ferroelectric liquid crystal [14]. According to Singh et al., a small amount of Ag-NPs dispersed at the room-temperature in NLC raised the threshold voltage and lowered the nematic–isotropic transition temperature [15]. The silver nanoparticle doped liquid crystal at low concentrations lead to a decrease in anisotropy as well as the threshold voltage [16]. Mishra et al. reported decrease in dielectric anisotropy by doping of gold

nanoparticles[17]. The present work is focused on the experimental results of an impact of dispersion of Ag-NPs in various concentrations (0.2, 0.4, 0.6, and 0.8 wt%) with host nematic NLCs 7CB will affect the dielectric permittivity(ε'), dielectric loss(ε") and dielectric strength (Δε).

2. Experimental

2.1 Materials and Sample preparations

The room temperature nematic liquid crystal material (7CB) with a purity 98%,used in this investigation was procured from Sigma-Aldrich, USA; the molecular mass and chemical formula are M_n = 277.4 g/mol and C_7H_{15} - C_6H_5 - C_6H_5 - CN respectively. A rod-like shaped with a length of 18.7Å and molecular structure of 7CB NLC is given below.

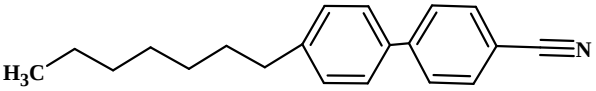

Figure: 1. Molecular structure of 7CB NLCs

The Ag-NPs with 99.9% purity were procured from NANOSHEL, USA with average particles size 30-50 nm. The NLC- nanoparticle composites were prepared by adding 0.2, 0.4, 0.6 and 0.8wt% of Ag-NPs into the NLC. Semi microbalance of WENSAR (MAB 250) was used for the weighing of the samples. Ag-NPs doped NLC was ultrasonicated in the isotropic phase of LC for 120 minutes using multifunctional ultrasonic cleaner (Athena tech) to achieve uniform dispersion

2.2 Instrument and Measurement techniques of material parameter

For dielectric measurement, N4L impedance analyzer (PSM3750) with IAI2 interface was used in the frequency range 100Hz to 10 MHz controlled by PSCOM2.V1 software. The sample temperature was controlled by using hot stage INSTEC HCS-302 connected with temperature controller mK2000 interfaced with INSTEC app software. To calculate the dielectric parameters (permittivity and loss) of the sample materials from measured impedance data it was mandatory for calibration of the cell and find out the active cell capacitance of the vacant cell. The capacitance of the vacant cell is

$$C_{air} = C_A + C_D \quad (1)$$

Where, C_A denotes the active and C_D is dead capacitance of the cell. The standard non-polar liquid (cyclohexane in this case) is filling into the cell for measurement of the active capacitance (C_A). The cyclohexane-filled cell's capacitance is :

$$C_{ch} = C_A\varepsilon'_{ch} + C_D \quad (2)$$

Here, $\varepsilon'(ch)$ is the relative dielectric permittivity of media (i.e., cyclohexane) at measured temperature.

From equation (1) and (2) gives out-

$$C_A = \frac{[C_{ch} - C_{air}]}{[\varepsilon'_{ch} - 1]} \quad (3)$$

The dielectric permittivity (ε') and dielectric loss (ε'') was determined by the equations;

$$\varepsilon' = \left[\frac{(C_m - C_{air})}{C_A}\right] + 1 \quad (4)$$

Since the cell (purchased from Instec) has etched sides and a well defined area so dead capacitance may not be as significant and, as a result:

$$\varepsilon' = \frac{C_m}{C_A} \quad (5)$$

where, C_m is the material filled capacitance of the cell. The dielectric absorption (loss) of the material filled cell is calculated with the help of equation of (5) and measured parameter from impedance analyzer (LCR meter):

$$\varepsilon'' = \frac{1}{2\pi f R C_0} = \varepsilon' \tan\delta \tag{6}$$

where, f is the frequency, R is the resistance of the material filled cell and C_0 is the free space capacitance of the active cell.

3. Results and discussion

Dielectric spectral analysis is an essential tool for understanding the molecular structure and dynamics of the molecules. It deals with the molecular mechanism response, which has a strong connection to the material's macroscopic polarization. The impedance spectroscopy of pure NLC and Ag-NPs dispersed NLC was carried out in a frequency range of 100Hz to 10 MHz using an N4L impedance analyzer. At low frequencies (< 100 Hz) and very high frequencies (>10 MHz) data obtained from the impedance analyzer suffers from some scarceness. To remove this scarceness, we fitted the data by using low frequency correction (LFC) for measured data. The frequency range from 100Hz to 10MHz endures minimum for NLCs. To analyze the observed data with theoretical concept, a generalized Cole-Cole equation was used for the fitting of dielectric graph[15,18,19].

$$\varepsilon^* = \varepsilon'(f) - j\varepsilon''(f) = \varepsilon'(\infty) + \sum \frac{(\delta\varepsilon')}{1 + j(f/f_r)^{(1-h)}} + \frac{A_1}{f^n} - j\frac{\sigma_{ion}}{2\pi f^k \varepsilon_0} - jA_2 f^m \tag{7}$$

From equation (7), measured complex permittivity (ε^*) have components as real (ε') and imaginary (ε'') part can be written as

$$\varepsilon'(f) = \varepsilon'(\infty) + \sum \frac{\delta\varepsilon\left\{1 + (f/f_r)^{(1-h)}\sin(h\pi/2)\right\}}{\left\{1 + (f/f_r)^{2(1-h)} + 2(f/f_r)^{(1-h)}\sin(h\pi/2)\right\}} + \frac{A_1}{f^n} \tag{8}$$

$$\varepsilon''(f) = \sum \frac{\delta\varepsilon(f/f_r)^{(1-h)}\cos(h\pi/2)}{1 + (f/f_r)^{2(1-h)} + 2(f/f_r)^{(1-h)}\sin(h\pi/2)} + \frac{\sigma_{ion}}{2\pi f^k \varepsilon_0} + A_2 f^m \tag{9}$$

where, $\delta\varepsilon = \varepsilon'(0) - \varepsilon'(\infty)$, f_r and h are the dielectric strength, the relaxation frequency and the distribution parameter ($0 \leq h \leq 1$), respectively. The dielectric permittivity $\varepsilon'(0)$ and $\varepsilon'(\infty)$ represent the relative dielectric permittivity at low and high frequency limits respectively. In equation (7) and (8), the third term shows the contribution of the electrode polarization of capacitance at low frequency value[20] where, *A* and *n* are the fitting parameters. The term $\frac{\sigma_{ion}}{2\pi\varepsilon_0 f^k}$ accounts for the contribution owing to ionic conductivity (σ_{ion}), with *k* as a fitting parameter and its value generally one for dc conductivity, and ε_0(=8.85pFm^{-1}) is the permittivity of free space. Equation (9) with A_2 and *m* serving as fitting constants as long as the correction term is small, adds an imaginary term ($A_2 f^m$) to partially account for the high frequency parasitic effects caused by ITO sheet resistance and lead inductance.

The measured permittivity (ε') and loss (ε'') data have been fitted using software (Origin pro8.5) separately using equation (8) and (9) to examine the relaxation mode and find the associated parameters. The various constants of equation (8) and (9) are determined through fitting of curve at high and low frequency parasitic correction terms are thus evaluated. Actual (corrected) dielectric spectra for the material are obtained by the subtracting the parasitic effects. Fig. 2 shows the variations of the dielectric permittivity and loss for the 0.2 wt% Ag-NPs at temperature 35 °C for the planar aligned sample with correction terms obtained by fitting it to generalized Cole-Cole equation [19,21] .

Industrial Engineering Journal
ISSN: 0970-2555
Volume : 53, Issue 11, No.1, November : 2024

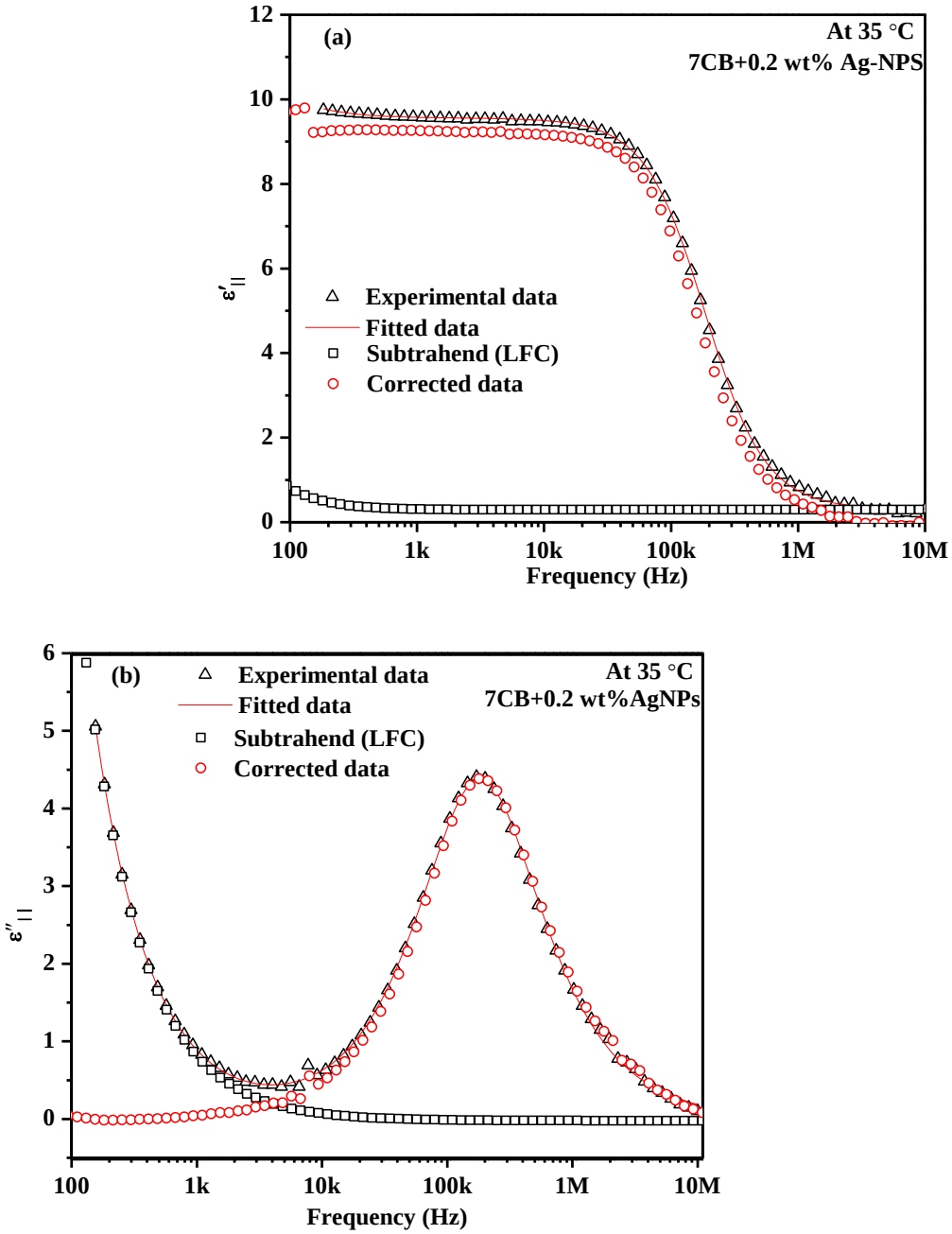

Figure: 2 Variations of dielectric permittivity and dielectric loss with frequency for 0.2 wt% Ag-NPs dispersed in 7CB NLCs at temperature 35 °C in vertical aligned sample (a) Dielectric permittivity ($\varepsilon'_{\parallel}$) and (b) Dielectric loss ($\varepsilon''_{\parallel}$) . The solid line with experimental data in (a) and (b) is best fit of Cole –Cole equation: low frequencies corrections term (LFC) and corrected data are shown in same figure to visualize the quality of fitting.

Fig.3 (a) shows the variations of transverse components (normal to the long axes of the molecules) of dielectric permittivity ($\varepsilon'_{\perp}$) with frequency for the pure and Ag-NPs (0.2, 0.4, 0.6, and 0.8 wt% concentrations) dispersed in a 7CB liquid crystal for Planar-aligned cell at 35 ^{0}C. In Fig.3 (b), at temperature 35° C, similar inclination of the variation of permittivity ($\varepsilon'_{\parallel}$) with frequency has been observed for vertical aligned sample. The maximum value of permittivity is observed for 0.2 wt% composite. The composites with higher dopant concentration, the permittivity is observed to decrease for higher concentrations. At the mid frequency region (1 kHz- 100 kHz) in Fig.3(b), the values of permittivity for 0.2 to 0.6 wt% Ag-NPs in the host material are higher than that of pure NLC whereas dispersed with 0.8 wt% Ag-NPs are slightly less than that of pure 7CB NLCs.

Industrial Engineering Journal
ISSN: 0970-2555
Volume : 53, Issue 11, No.1, November : 2024

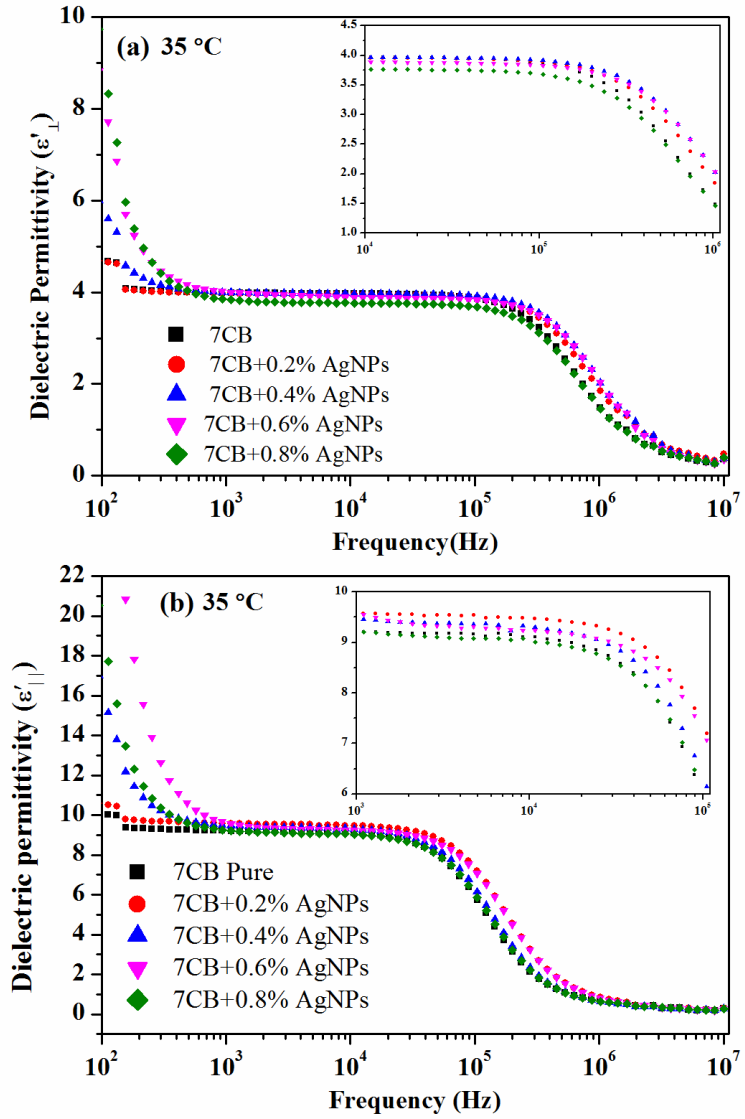

Figure 3: Variations of dielectric permittivity (transverse component ε'⊥ and parallel component ε'∥) with frequency in (a) Planar and (b) Homeotropic alignment of pure and Ag-NPs doped 7CB LC at 35^0C.

From Fig.3, it is clear that the curves in the mid-frequency region (1 kHz to 100 kHz), are almost parallel to the y-axis, i.e., permittivity remains unchanged for all composites. The value of permittivity ($\varepsilon'_{\perp}$) less than 1 KHz is affected by ionic effect[22] whereas the frequency region in MHz, high- frequency parasitic effect dominates[23]. Ionic effect[22] increases with the concentration of NPs up to 0.6wt%. Agglomeration starts due higher concentration of NPs so the permittivity decreases. It is important to add that the measured dielectric data are affected by the parasitic effects[24] at low and high frequencies hence to remove them from data fitted with generalized Cole-Cole equations. From Fig.3, it is clear that the magnitude of parallel component of dielectric permittivity is greater than vertical component confirming the positive dielectric anisotropy in both 7CB and its composites.

Fig. 4 (a) and (b) shows the variation of dielectric loss as a function of frequency for pristine and Ag-NPs doped in 7CB liquid crystal of planar aligned and vertical aligned sample at 35°C.

Industrial Engineering Journal
ISSN: 0970-2555
Volume : 53, Issue 11, No.1, November : 2024

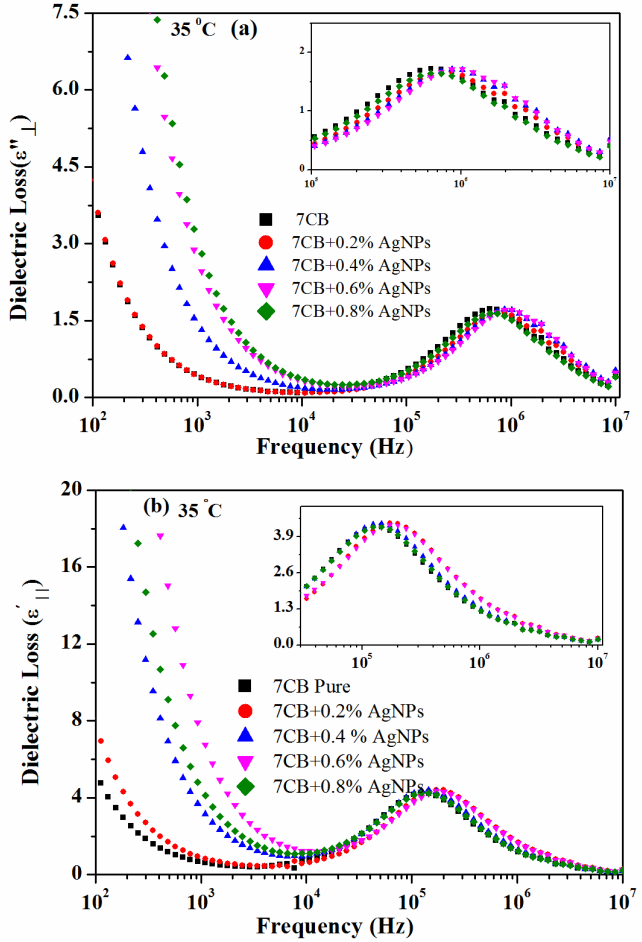

Figure 4: Variations of dielectric loss with frequency for pure and Ag-NPs dispersed in 7CB liquid (a) transverse component ($\varepsilon''_{\perp}$) and (b) longitudinal component ($\varepsilon''_{\parallel}$). at 35°C.

The imaginary part of perpendicular and parallel dielectric constants indicates a dielectric relaxation peak [25]. Fig. 4 (a) shows a relaxation mechanism between 100 kHz to 1MHz frequency region in the case of planar-aligned molecules. Above 10 MHz, any relaxation mechanism resulting from molecules rotating around their short axes (planar-aligned molecules) take place. Actually, the cell's parasitic effect essentially causes the observed pseudo-relaxation mechanism [23,26]. It is dependent upon the cell's electrode resistance, lead inductance and capacitance all working together [23]. In the Fig 4(a), the relaxation frequency (f_r) for pure 7CB LCs was found to be 700kHz. Moreover, the relaxation frequencies for other concentrations i.e. 0.2, 0.4, and 0.6 wt% Ag-NPs were found 853 kHz, 1MHz and 1.03 MHz respectively. Clearly, the relaxation frequency increases from pure to 0.6wt% and hence, the relaxation time decreased for dispersed system. For 0.8wt% it is decreased. The relaxation frequency f_r for 7CB LCs was found to be 123 kHz in vertical aligned sample cell shown in Fig.4 (b). In addition, it was found to be 170 kHz for 0.2 and 0.6 wt% Ag-NPS dispersed system and 145 kHz for 0.4 and 0.8 wt% of Ag-NPs system. It indicates that relaxation frequency of dispersed system was shifted towards the high frequency region. The molecules ability to rotate is also hindered by Ag-NPs. Thus, compared with pure sample, the relaxation frequency is increased. On the other hands, the size and concentration of the NPs had a significant impact on the reorientation of the LC molecules. Additionally, it is dependent on the applied AC field [27,28]. In Fig 4(a), it has been observed here that in lower frequency region, the dielectric loss gets almost same for pristine and 0.2 wt % doped LCs and increases for other concentration (0.4, 0.6, and 0.8 wt%) Ag-NPs dispersed LCs. In Fig. 4(b), for vertical aligned cell, the dielectric loss for Ag-NPs dispersed LCs was increased from the pure 7CB LC. The maximum value of dielectric loss occurs in both Planar and vertically aligned sample at the lower frequency region (30 kHz to 100 Hz) due to

effect of ionic charges [22]. At the frequency region 10 kHz to 100 kHz, the dielectric losses were found to be minimum value for a pure 7CB and Ag-NPs dispersed system.

A Cole-Cole plot between dielectric permittivity and loss after low frequency correction for pure and different concentrations is shown in Fig. 5 (a) and (b). All the curves shows the almost semi-circle suggested the relaxation mechanism of the Debye processes [19,24]. From figure 5, it shows the relaxation frequency for pure 7CB is 0.7 MHz and it was increased for the concentrations of 0.2, 0,4, and 0,6 wt% of Ag-NPs dispersed in 7CB. For concentration of 0.8 wt% of Ag-NPs, relaxation frequency was decreased from other concentration but it is also greater for pure 7CB. This is due to the increase in availability of the volume for molecular motion because of the presence of spherical Ag-NPs[15,27]

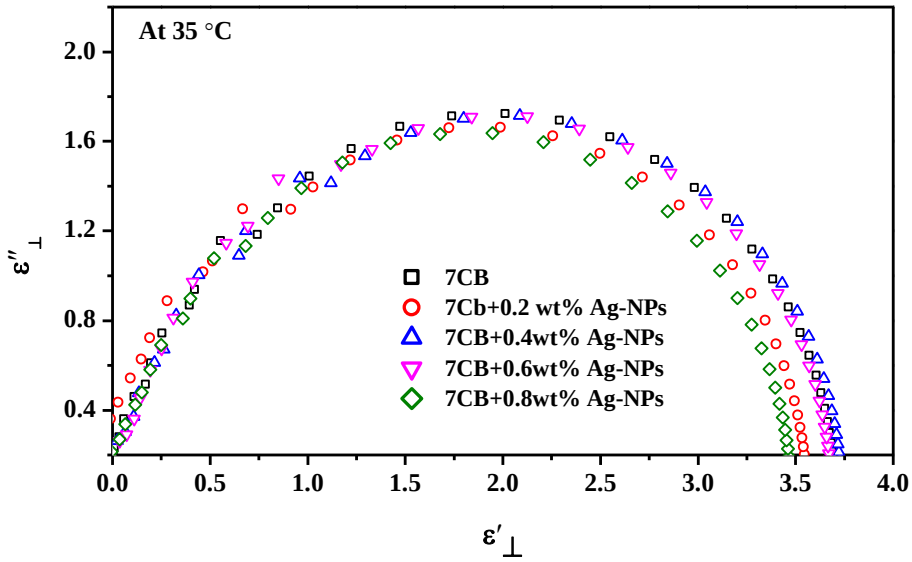

Figure 5: The Cole-Cole plots of observed relaxation mode in planar aligned sample for pure 7CB and Ag-NPs for concentrations 0f 0.2, 0.4, 0.6 and 0.8 wt% at temperature 35°C.

Fig. 6 and 7 shows the variations of the dielectric strength and the relaxation frequency between wt % Ag-NPs concentrations in host nematic LCs at fixed temperature 35°C. From fig.6, it is clear that the dielectric strength of the 0.8 wt% Ag-NPs dispersed LC is lower in comparison of the other concentrations.

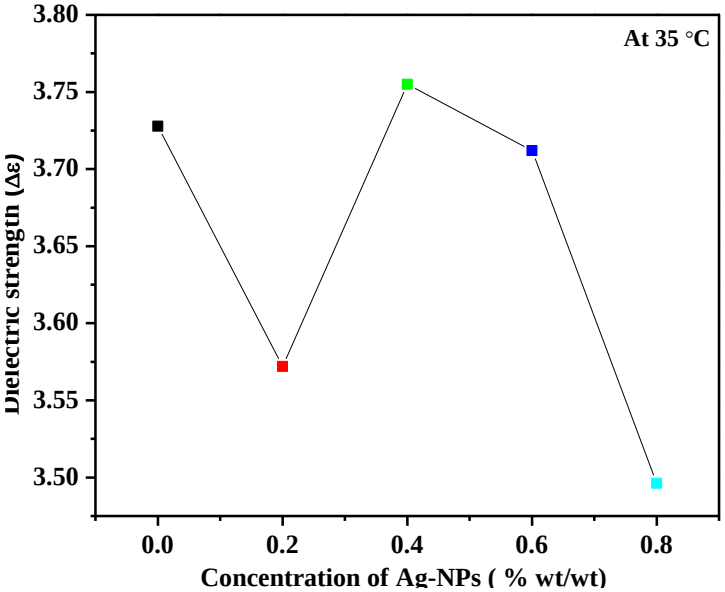

Figure 6: Variations of the dielectric strength with the concentration of the pure And Ag-NPs dispersed LC at the temperature 35 °C.

Relaxation frequency is the essential parameter for the display devices which is related with inverse of the relaxation time (τ_0), which measures the time limit required to reorientation of the molecules. Higher relaxation frequency of the doped LC increases from the pure LC. The relaxation time was decreased for the Ag-NPs doped LCs.

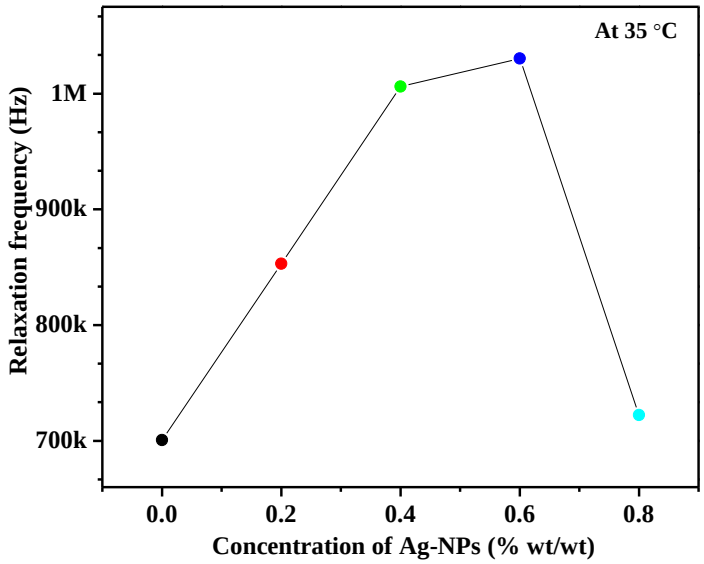

Figure 7: Variations of the relaxation frequency with the concentration of the Ag-NPs dispersed LCs.

4. Conclusion:

From the above mentioned results and discussion, it is conclude that due to the dispersion of Ag-NPs, the dielectric permittivity for the Ag-NPs dispersed LC (0.2. 0.4, and 0.6 wt%) was improved from the pure 7CB LCs where as for the concentration of the 0.8 wt% Ag-NPs dispersed LC it was decreased due to the agglomerations of the Ag-NPs molecule surrounding with LC molecules. The dielectric strength for the concentration 0.2 wt% and 0.8% was decreased from the pure 7CB LCs. The relaxation frequency for Ag-NPs doped LC was increased from the pure 7CB LC shows the relaxation time was decreased which is improvement of the display parameters.

Acknowledgements

Authors (Dr. Anil Kumar, Dr Sindhu Singh and Dr. Anoop K Srivastava) are Thankful to Department Higher Education, U.P. Government for financial support under Centre of Excellence and Research & Development Grant.

References

[1] Collings, P.J.; Hird, M. Introduction to Liquid Crystals Chemistry and Physics, Taylor& Francis. 2009, 1-295.

[2] Andrienko, D. Introduction to liquid crystals, Journal of Molecular Liquids. 2018, 267, 520–541.

[3] Maurya, A.; Awasthi, D.K. An Introduction to Liquid Crystals and It's Types Nematic, Smetic and Cholestric Crystals, International Research Journal of Innovations in Engineering and Technology. 2022, 6, 101.

[4] Tripathi, P.K.; Singh, D.P.; Yadav,T.; Singh,V.; Srivastava, A.K.; Negi,Y.S. Enhancement of birefringence for liquid crystal with the doping of ferric oxide nanoparticles, Optical Materials. 2023, 135, 113298.

[5] Al-Hazmi, F.; Al-Ghamdi, A.A.; Al-Senany,N.; Alnowaiser, F.; Yakuphanoglu, F. Dielectric anisotropy and electrical properties of the copper phthalocyanine (CuPc): 4–4′-n-

Heptylcyanobiphenyl (7CB) composite liquid crystals, Composites Part B: Engineering 2014, 56 ,15–19.
[6] Shehzad,K.; Hussain,T.; Shah, A.T.; Mujahid, A.; Ahmad, M.N.; Sagar,R.U.R.; Anwar, T.; Nasir,S.; Ali, A. Effect of the carbon nanotube size dispersity on the electrical properties and pressure sensing of the polymer composites. J Mater Sci. 2016, 51, 11014–11020.
[7] Mirzaei, J.; Reznikov, M.; Hegmann, T. Quantum dots as liquid crystal dopants. Journal of Materials Chemistry. 2012, 22, 22350–22365.
[8] Kato, T.; Mizoshita, N.; Kishimoto, K. Functional Liquid Crystalline Assemblies: Self Organized Soft Materials, Angew Chem Int Ed. 2006, 45, 38–68.
[9] Singh,D. P. Liquid Crystal- Nanomaterial Composite Systems, University Of Lucknow, 2015.
[10] Gorkunov, M.; Osipov, M. Mean-field theory of a nematic liquid crystal doped with anisotropic nanoparticles, Soft Matter 2011, 7 , 4348–4356.
[11] Qi, H.; Hegmann, T. Impact of nanoscale particles and carbon nanotubes on current and future generations of liquid crystal displays, Journal of Materials Chemistry. 2008, 18, 3288–3294.
[12] Ahmad,F.; Luqman, M.; Jamil, M. Advances in the metal nanoparticles (MNPs) doped liquid crystals and polymer dispersed liquid crystal (PDLC) composites and their applications - a review, Molecular Crystals and Liquid Crystals 2021, 731, 1–33.
[13] Haynes, C.L.; McFarland, A.D.; Zhao, L.; Van Duyne, R.P.; Schatz, G.C; Gunnarsson, L.; Prikulis, Kasemo, J. B.; Käll, M. Nanoparticle Optics: The Importance of Radiative Dipole Coupling in Two-Dimensional Nanoparticle Arrays, J. Phys. Chem. B. 2003, 107, 7337–7342.
[14] Vimal, T.; Gupta, S. K.; Katiyar, R.; Srivastava, A.; Czerwinski, M.; Krup, K.; Kumar,S.; Manohar, R. Effect of metallic silver nanoparticles on the alignment and relaxation behaviour of liquid crystalline material in smectic C* phase. Journal of Applied Physics. 2017, 122.
[15] Singh, U.B.; Dhar, R.; Dabrowski, R.; Pandey, M.B. Influence of low concentration silver nanoparticles on the electrical and electro-optical parameters of nematic liquid crystals. Liquid Crystals. 2013, 40, 774–782.
[16] Tripathi, P.; Mishra, M.; Kumar, S.; Dabrowski, R.; Dhar, R. Dependence of physical parameters on the size of silver nano particles forming composites with a nematic liquid crystalline material. Journal of Molecular Liquids. 2018, 268, 403–409.
[17] Mishra, M.; Kumar, S.; Dhar, R. Effect of high concentration of colloidal gold nanoparticles on the thermodynamic, optical, and electrical properties of 2, 3, 6, 7, 10, 11-hexabutyloxytryphenylene discotic liquid crystalline material. Soft Materials. 2017, 15, 34–44.
[18] Verma, R.; Mishra, M.; Dhar, R.; Dabrowski, R. Enhancement of electrical conductivity, director relaxation frequency and slope of electro-optical characteristics in the composites of single-walled carbon nanotubes and a strongly polar nematic liquid crystal, Liquid Crystals 2017, 44, 544–556.
[19] Cole, K.S.; Cole, R.H. Dispersion and Absorption in Dielectrics I. Alternating Current Characteristics. The Journal of Chemical Physics. 1941, 9, 341–351.
[20] Kumar, A.; Dhar, R.; Agrawal, V.K.; Dabrowski, R. Thermodynamic and dielectric studies on antiferroelectric liquid crystal (***S***)-4-(1-methylheptyloxycarbonyl) phenyl 4-(6-heptanoyloxyhex-1-oxy)biphenylate. Phase Transitions. 2007, 80, 231–241.
[21] Verma, H. Lal, A.; Singh, P.K.; Pandey, M.B.; Dabrowski, R.; Dhar, R. Silver nanoparticles induced enhanced stability, dielectric anisotropy, and electro-optical parameters of a nematic liquid crystalline material 4-(trans-4-n-hexylcyclohexyl) isothiocyanatobenzene. Journal of Molecular Liquids . 2024, 400, 124503.
[22] Srivastava, SL.; Dhar, R. Characteristic time of ionic conductance and electrode polarization capacitance in some organic liquids by low frequency dielectric spectroscopy. Indian Journal of Pure & Applied Physics. 1991, 29, 745–751.

[23] Dhar, R. An impedance model to improve the higher frequency limit of electrical measurements on the capacitor cell made from electrodes of finite resistances. Indian Journal of Pure & Applied Physics. 2004 . 42,.
[24] Dhar,; R. Comments on the fitting of Cole-Cole/Havriliak-Negami equation with the dielectric data under the influence of parasitic effects in order to extract correct parameters of the materials. Journal of Molecular Liquids. 2021, 343, 117682.
[25] Al-Hazmi, F.; Al-Ghamdi, A.; Senany, A. N.; Alnowaiser, F.; Yakuphanoglu, F. Dielectric anisotropy and electrical properties of the copper phthalocyanine (CuPc): 4–4′-n-Heptylcyanobiphenyl (7CB) composite liquid crystals, Composites Part B: Engineering , 2014 , 56, 15–19.
[26] Pandey,F.P.; Rastogi, A.; Manohar, R.; Dhar, R.; Singh, S. Dielectric and electro-optical properties of zinc ferrite nanoparticles dispersed nematic liquid crystal 4’-Heptyl-4-biphenylcarbonnitrile. Liquid Crystals. 2020, 47, 1025–1040.
[27] Vardanyan, K.K.; Hecker, E. Influence of the dispersed silver nanoparticles size and concentration on the properties of 6CB nematic. Liquid Crystals. 2023, 1–15.
[28] Dixit, A.C.; Pandey, K.; Tripathi, P.K.; Khan, M.S. Dielectric Study of Carbon Nanotube Dispersed Thermotropic Liquid Crystal. Int. J. Nanotec. Appl. 2017, 11, 179–188.